

20. C. B. F. Andersen *et al.*, *Science* **313**, 1968 (2006); published online 23 August 2006 (10.1126/science.1131981).
21. K. J. Marians, *Structure* **5**, 1129 (1997).
22. S. Korolev, N. Yao, T. M. Lohman, P. C. Weber, G. Waksman, *Protein Sci.* **7**, 605 (1998).
23. E. J. Tomko, C. J. Fischer, A. Niedziela-Majka, T. M. Lohman, *Mol. Cell* **26**, 335 (2007).
24. M. Houghton, A. Weiner, J. Han, G. Kuo, Q. L. Choo, *Hepatology* **14**, 381 (1991).
25. S. Myong, I. Rasnik, C. Joo, T. M. Lohman, T. Ha, *Nature* **437**, 1321 (2005).
26. We thank C. Joo for help in manuscript preparation. Supported by NIH grants R01-GM060620 and R01-GM065367. T.H. and A.M.P. are investigators with the Howard Hughes Medical Institute.

Supporting Online Materialwww.sciencemag.org/cgi/content/full/317/5837/513/DC1

Materials and Methods

Figs. S1 to S9

Movie S1

23 April 2007; accepted 26 June 2007

10.1126/science.1144130

Sirtuin 2 Inhibitors Rescue α -Synuclein–Mediated Toxicity in Models of Parkinson’s Disease

Tiago Fleming Outeiro,^{1,2} Irene Kontopoulos,^{3*} Stephen M. Altmann,^{2*} Irina Kufareva,⁴ Katherine E. Strathearn,⁵ Allison M. Amore,² Catherine B. Volk,⁵ Michele M. Maxwell,² Jean-Christophe Rochet,⁵ Pamela J. McLean,^{1,2} Anne B. Young,² Ruben Abagyan,⁴ Mel B. Feany,³ Bradley T. Hyman,^{1,2} Aleksey G. Kazantsev^{2†}

The sirtuins are members of the histone deacetylase family of proteins that participate in a variety of cellular functions and play a role in aging. We identified a potent inhibitor of sirtuin 2 (SIRT2) and found that inhibition of SIRT2 rescued α -synuclein toxicity and modified inclusion morphology in a cellular model of Parkinson’s disease. Genetic inhibition of SIRT2 via small interfering RNA similarly rescued α -synuclein toxicity. Furthermore, the inhibitors protected against dopaminergic cell death both in vitro and in a *Drosophila* model of Parkinson’s disease. The results suggest a link between neurodegeneration and aging.

Aging is a major risk factor for the development of several neurodegenerative diseases, including Parkinson’s disease (PD). Although the molecular basis of aging is yet to be determined, biological pathways involved in aging may provide targets for therapeutic intervention in neurodegeneration. PD causes loss of dopaminergic neurons and development of Lewy bodies containing α -synuclein (α -Syn) in the substantia nigra (1). Allele multiplication and mutations link α -Syn to familial forms of PD (2).

Silent information regulator 2 (Sir2), a nicotinamide adenine dinucleotide-dependent histone deacetylase (HDAC) in yeast, participates in numerous cell functions including cell protection and cell cycle regulation (3). The sirtuins are evolutionarily conserved, and seven distinct sirtuin proteins, SIRT1 to SIRT7, have been identified in humans. The mammalian ortholog of yeast Sir2, SIRT1, is up-regulated under conditions of caloric

restriction and resveratrol treatment and is predicted to have a role in cell survival (4). Human SIRT2 is involved in cell cycle regulation via the deacetylation of α -tubulin (5). However, the iden-

tification of p53 and histones H3 and H4 as additional substrates for SIRT2 suggests a broader regulatory role in the cell (6, 7). Small-molecule inhibitors targeting HDACs ameliorate several models of neurodegeneration (8).

Compound B2 is associated with an increase in intracellular α -Syn inclusion size from numerous small aggregates to larger inclusions (9). B2 activity was examined in a panel of cell-free enzymatic assays including HDAC I and II; SIRT1, 2, and 3; caspase 1 and 6; β -site amyloid precursor protein cleaving enzyme-1 (BACE1); calpain; cathepsin H, L, and S; and molecular chaperones Hsp70 and Hsp27. The only activity detected was a weak [median inhibitory concentration (IC_{50}) = 35 μ M], but consistent, selective inhibition of SIRT2 (Fig. 1, A and B, and fig. S1). To determine the relevance of SIRT2 inhibition, we used a targeted knockdown approach. Human neuroglioma cells (H4) were cotransfected with α -Syn expression constructs and synthetic small interfering RNA (siRNA) against either SIRT2 or SIRT3 for 24 hours and were then assessed for cytotoxicity. Rescue of α -Syn-mediated toxicity was observed only in cells receiving the SIRT2

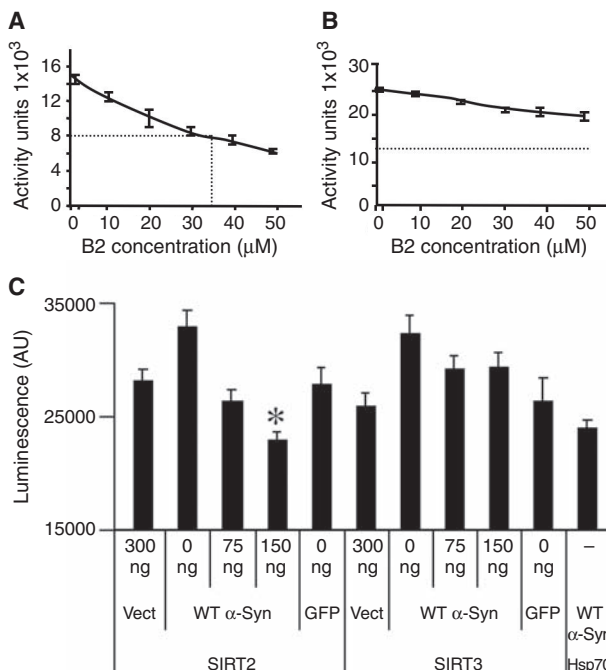


Fig. 1. Inhibition of SIRT2 modulates α -Syn toxicity. (A and B) B2 biochemical activity profiles against SIRT2 (A) and SIRT3 (B) in an in vitro deacetylation biochemical assay containing recombinant SIRT proteins. (C) α -Syn-mediated toxicity can be rescued with SIRT2 siRNA and Hsp70 overexpression but not with SIRT3 siRNA in vitro (t test, $n = 3$, $*P < 0.005$).

*These authors contributed equally to this work.

†To whom correspondence should be addressed. E-mail: akazantsev@partners.org

siRNA (Fig. 1C). A comparable rescue of α -Syn-mediated toxicity was achieved with Hsp70 overexpression (Fig. 1C).

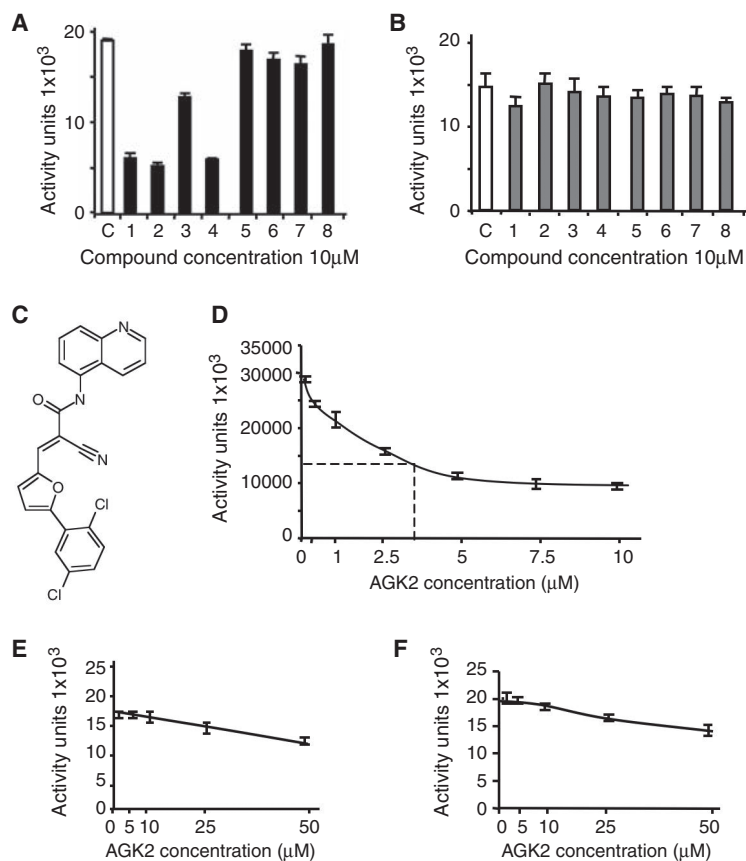


Fig. 2. Identification of a potent and selective SIRT2 inhibitor. **(A and B)** Effect of eight representative compounds (out of 200) from a focused B2 library against SIRT2 (A) and SIRT3 (B) activity identifies compound 2 (AGK2) as the most potent against SIRT2. A single-dose (10 μ M) primary screen was conducted for each compound, using an in vitro SIRT2 biochemical assay. C is DMSO control. **(C and D)** Structure (C) and dose-response profile (D) of AGK2 in a SIRT2 enzymatic assay. **(E and F)** Dose-response inhibition profiles of AGK2 in SIRT1 (E) and SIRT3 (F) in an in vitro enzymatic assay.

Fig. 3. Validation of AGK2-mediated inhibition of SIRT2. **(A)** The ability of AGK2 to inhibit deacetylation of α -tubulin by SIRT2 was assessed via immunoblot using antibodies (Ab) to acetylated (top lanes) and total (bottom lanes) α -tubulin. The inactive compound AGK7 and the known SIRT2 inhibitor sirtinol were included as control compounds. **(B)** Effect of AGK2 on activity of over-expressed SIRT2 and SIRT3 immunoprecipitated from HeLa cells. **(C)** AGK2 treatment results in a dose-dependent increase in acetylation of soluble tubulin monomers (S) and polymerized microtubules (P) in fractionated HeLa cell extracts. The effect of the less potent SIRT2 inhibitor AGK3 is shown for comparison. **(D)** AGK2 has a minimal effect on cell viability after 72 hours. **(E)** Low-energy pose of AGK2 in SIRT2 generated by virtual ligand docking. Nicotinamide position is shown in wire for comparison.

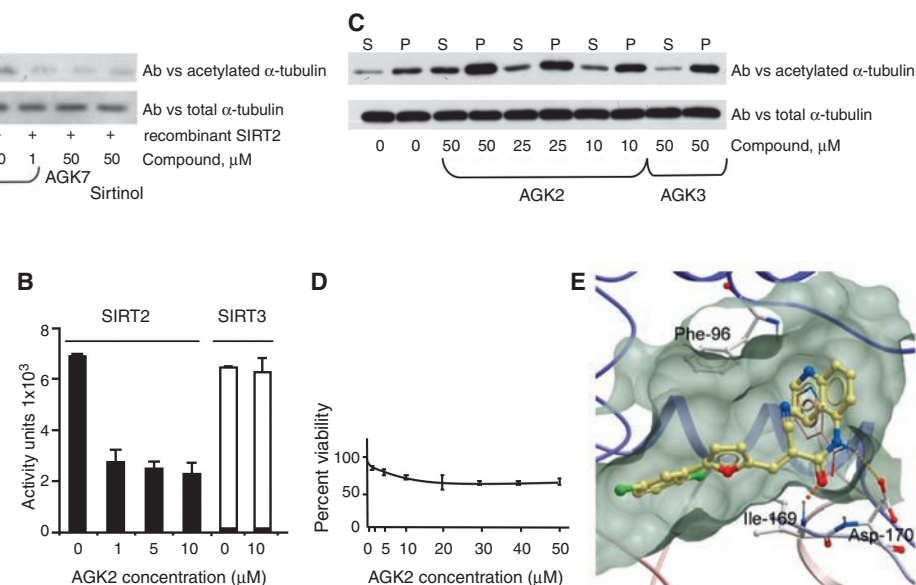
Next, we designed a library of 200 structural analogs of B2 and other previously identified aggregation modifiers. Screening the library by means

of SIRT2 (Fig. 2A) and SIRT3 (Fig. 2B) fluorometric assays revealed a promising lead series scaffold, AGK (fig. S1A). Inhibition profiles against human SIRT1, 2, and 3 were generated (figs. S2 and S3). The most potent inhibitor, AGK2 (Fig. 2C), had a calculated IC₅₀ for SIRT2 of 3.5 μ M, representing a factor of 10 increase in potency over B2 (Fig. 2D). By contrast, a slight inhibition of SIRT1 and 3 was observed only at concentrations over 40 μ M (Fig. 2, E and F), indicating that AGK2 was a potent and selective inhibitor of SIRT2. Additional selective lower-potency SIRT2 inhibitors were identified (figs. S2 and S3).

SIRT2 preferentially deacetylates α -tubulin at Lys⁴⁰ in both purified tubulin heterodimers and taxol-stabilized microtubules (5). To determine whether AGK2 could inhibit the deacetylation activity of SIRT2 against a native substrate, we used tubulin heterodimers purified from bovine brain. Treatment with AGK2 led to an increase in acetylated tubulin relative to an inactive control, AGK7, and the known SIRT2 inhibitor sirtinol (Fig. 3A). Only one other compound from a different structural scaffold, AK-1, resulted in increased acetylation in this assay, indicating its stringent specificity (fig. S3D).

To determine whether AGK2 inhibited SIRT2 activity in human cells, we transfected HeLa cells with a SIRT2-myc expression construct. Immunoprecipitated SIRT2 was then used in the enzyme assay, with or without AGK2. As anticipated, AGK2 was effective in inhibiting the activity of SIRT2-myc; hence, the activity of AGK2 was not limited to recombinant SIRT2 but was also effective against SIRT2 that had been folded and processed by the intracellular machinery (Fig. 3B). A comparable assay using immunoprecipitated SIRT3 showed no inhibition by AGK2.

We next examined insoluble, polymerized microtubules and soluble α -tubulin after treatment of HeLa cells with either AGK2 or AGK3, a less potent structural analog of AGK2, for 3 hours. A dose-dependent increase in acetylated



tubulin was observed in both fractions of AGK2-treated cells relative to untreated or AGK3-treated cells (Fig. 3C). Thus, AGK2 could enter cells and act on endogenous SIRT2 in its native environment. By contrast, AK-1 did not increase acetylated tubulin in live cells, which suggests that its lower potency was insufficient to produce a detectable effect in this particular assay. Incubation of HeLa cells with AGK2 for 72 hours resulted in only minimal toxicity at the higher compound concentrations (Fig. 3D).

To elucidate the structural mechanism of SIRT2 inhibition by AGK2 and AK-1, we developed models of human SIRT2 in several different conformations (10). Comparative analysis of the low-energy ligand conformations confirmed that the preferred site for ligand binding is the “C-pocket” (11). This hydrogen-bonding pattern mimics the effect of nicotinamide, a known inhibitor of sirtuins (11). Examples of the top-scoring poses for AGK2 and AK-1 are shown in Fig. 3E and fig. S4C, respectively.

For pharmacological validation of SIRT2 as a target in a PD functional assay, we transfected H4 cells with α -Syn or a control empty vector and treated them for 24 hours with AGK2, AK-1, AGK7, or dimethyl sulfoxide (DMSO). AGK2 reduced α -Syn-mediated toxicity in a dose-dependent manner, whereas the less potent AK-1 reduced α -Syn-mediated toxicity to a lesser extent and without clear dose dependency. By contrast, the inactive AGK7 had no effect (Fig. 4A).

To rule out other explanations for the alleviation of α -Syn toxicity, we examined levels of α -Syn as well as chaperones Hsp70 and Hsp27, which are known to rescue α -Syn-mediated toxicity (12, 13), after AGK2 treatment. We detected no change in α -Syn, Hsp70, or Hsp27 in the presence of AGK2. As a positive control, cells were treated with the Hsp90 inhibitor geldanamycin, which induces Hsp70 and prevents α -Syn-mediated toxicity in H4 cells (14).

To assess the effect of SIRT2 inhibition on α -Syn aggregation, we cotransfected H4 cells with α -Syn and synphilin-1, an established paradigm that leads to inclusion formation in H4 cells (15). After transfection, cells were treated with AGK2, AK-1, or AGK7 for 24 hours. When compared to DMSO-treated cells (Fig. 4C), the inactive AGK7 failed to affect α -Syn aggregation (Fig. 4D), whereas AGK2 and AK-1 promoted the formation of enlarged inclusions (Fig. 4, E and F), although AK-1 did so to a lesser extent.

To determine whether AGK2 and AK-1 protected dopaminergic neurons from α -Syn-induced toxicity, we examined α -SynA53T-dependent dopaminergic cell death in primary midbrain cultures. We focused our efforts on the α -SynA53T ($\text{Ala}^{53} \rightarrow \text{Thr}$) mutant because it is more toxic than wild-type α -Syn in this assay (16). Primary midbrain cultures were transduced with lentivirus encoding α -SynA53T with or without compounds B2, AK-1, or AGK2. Untransduced cells were treated with DMSO (0.2%, v/v) to control for nonspecific

toxicity. Cultures infected with A53T lentivirus had fewer tyrosine hydroxylase (TH)-positive neurons relative to cultures infected with A53T virus in the presence of B2, AK-1, or AGK2, which were similar to control, untransduced levels (Fig. 4G). Thus, B2, AK-1, or AGK2 rescued α -SynA53T-mediated dopaminergic cell death in this alternative model.

To validate the protective effects of AK-1 and AGK2 against α -Syn-mediated toxicity in vivo,

we used a *Drosophila* model of PD (17) where α -Syn, under the control of the upstream activating sequence for the yeast transcription factor GAL4, is directed to the fly brain via the *elav-GAL4* pan-neuronal driver. Transgenic flies were fed DMSO or increasing doses of AK-1 or AGK2 for the first 20 days of adult life. As expected, DMSO-fed flies exhibited a marked loss of TH-positive neurons in the dorsomedial cluster, the region that is sensitive to α -Syn-induced toxicity (17, 18). By contrast,

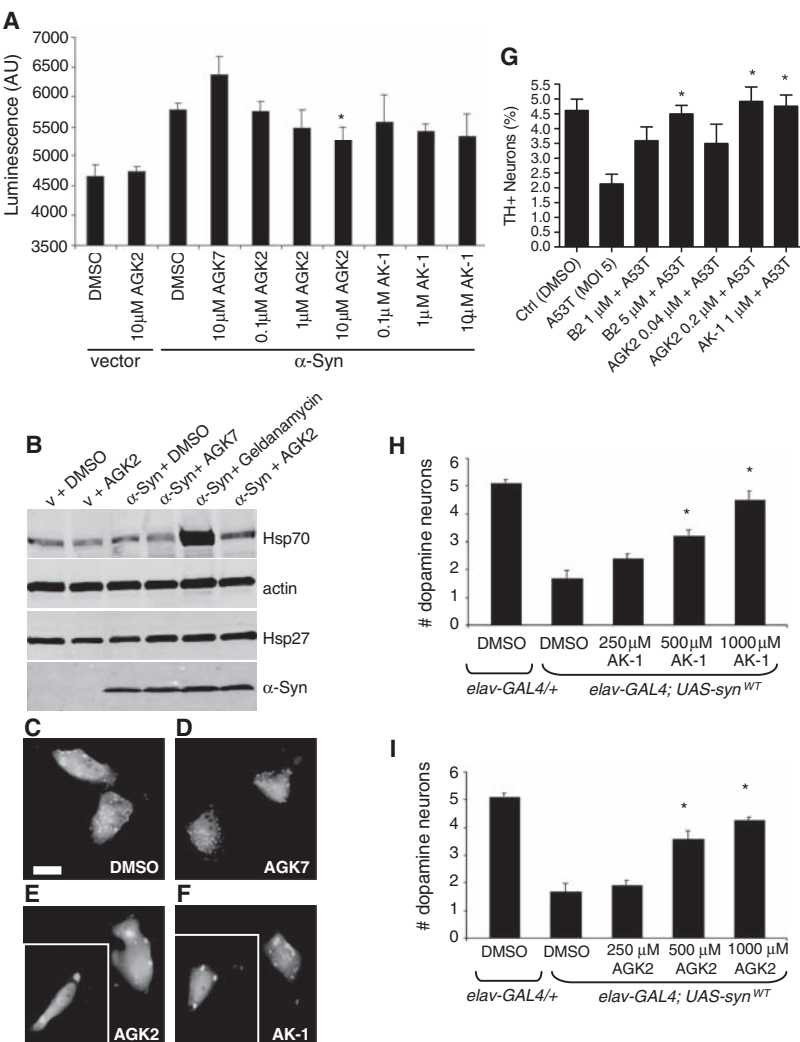


Fig. 4. SIRT2 inhibitors rescue α -Syn-mediated toxicity and modify aggregation in models of PD. **(A)** AGK2 reduces α -Syn-mediated toxicity in a dose-dependent manner as measured via release of adenylate kinase into cell culture media (paired *t* test, $n = 3$, $*P < 0.05$). The inactive compound AGK7 had no effect, and the less potent AK-1 is not dose-dependent. **(B)** AGK2 has no effect on Hsp70 or Hsp27 expression, whereas geldanamycin induces Hsp70 expression. V = empty vector. **(C to F)** α -Syn inclusions remain unaltered in DMSO (C) and the inactive compound AGK7 (D) but decrease in number and increase in size after treatment with AGK2 (E) or AK-1 (F) for 24 hours. Scale bar, 20 μm . **(G)** Primary midbrain cultures were transduced with α -SynA53T encoding lentivirus (multiplicity of infection = 5) in the presence of vehicle (DMSO) or increasing concentrations of B2, AGK2, or AK-1. Control cells were untransduced but treated with DMSO. Dopaminergic cell death was evaluated with antibodies to MAP2 and TH; viability is expressed as the percentage of MAP2-immunopositive cells that were also TH-immunonegative. Data are means \pm SEM, $N > 3$, $*P < 0.01$, one-way analysis of variance with Dunnett's multiple-comparison post hoc test (versus α -SynA53T alone). **(H and I)** Administration of AK-1 (H) or AGK2 (I) rescues α -Syn-mediated toxicity of dorsomedial dopamine neurons in 20-day-old wild-type transgenic flies in a dose-dependent manner ($*P < 0.01$). Animals were fed 250, 500, or 1000 μM AK-1 or AGK2 for 20 days.

transgenic flies fed increasing doses of either AK-1 or AGK2 had a striking dose-dependent rescue of dorsomedial neurons (Fig. 4, H and I). No change occurred in steady-state levels of α -Syn after administration of the SIRT2 inhibitors (fig. S5).

Rescue via inclusion enlargement, and the concomitant reduction in total surface area of inclusions, agrees with a cytoprotective role of aggregates (19) and suggests a mechanistic basis for the effect of SIRT2 inhibition—that it reduces aberrant interactions of aggregates with cellular proteins. Conceivably, coalescence of misfolded proteins into larger inclusions may lower the concentration of toxic, submicroscopic α -Syn oligomers, thereby leading to the rescue of proteome dysfunction. Indeed, the formation of large β -amyloid aggregates is protective against proteotoxicity in *Caenorhabditis elegans* (20).

The exact mechanism whereby SIRT2 inhibition affects α -Syn aggregation remains uncertain. Increased α -tubulin acetylation is associated with microtubule stabilization, and α -Syn has been reported to interact with α -tubulin as well as the microtubule-binding proteins MABP1 and tau (21, 22). One possibility is that the increase in acetylated α -tubulin resulting from SIRT2 inhibition may stimulate aggregation of α -Syn through its affinity to microtubules. Moreover, microtubule stabilization itself could be an important factor contributing to neuroprotection. A neuroprotective role for another microtubule

deacetylase, HDAC6, was recently proposed, although the protective mechanism is unclear (23–25).

Our data are consistent with the recent observation that α -Syn-dependent inhibition of histone acetylation is associated with increased neurotoxicity (4). Thus, SIRT2 targeting may be therapeutically beneficial in other diseases where aggregation of misfolded proteins is central to disease pathogenesis.

References and Notes

- M. G. Spillantini *et al.*, *Nature* **388**, 839 (1997).
- A. B. Singleton *et al.*, *Science* **302**, 841 (2003).
- G. Blander, L. Guarente, *Annu. Rev. Biochem.* **73**, 417 (2004).
- E. Kontopoulos, J. D. Parvin, M. B. Feany, *Hum. Mol. Genet.* **15**, 3012 (2006).
- B. J. North, B. L. Marshall, M. T. Borra, J. M. Denu, E. Verdin, *Mol. Cell* **11**, 437 (2003).
- B. Heltweg *et al.*, *Cancer Res.* **66**, 4368 (2006).
- A. Vaquero *et al.*, *Genes Dev.* **20**, 1256 (2006).
- B. Langley, J. M. Gensert, M. F. Beal, R. R. Ratan, *Curr. Drug Targets CNS Neural. Disord.* **4**, 41 (2005).
- R. A. Bodner *et al.*, *Proc. Natl. Acad. Sci. U.S.A.* **103**, 4246 (2006).
- R. Abagyan, M. Totrov, D. Kuznetsov, *J. Comput. Chem.* **15**, 488 (1994).
- J. L. Avalos, K. M. Bever, C. Wolberger, *Mol. Cell* **17**, 855 (2005).
- J. Klucken, Y. Shin, E. Masliah, B. T. Hyman, P. J. McLean, *J. Biol. Chem.* **279**, 25497 (2004).
- T. F. Outeiro *et al.*, *Biochem. Biophys. Res. Commun.* **351**, 631 (2006).
- P. J. McLean *et al.*, *J. Neurochem.* **83**, 846 (2002).
- P. J. McLean, H. Kawamata, B. T. Hyman, *Neuroscience* **104**, 901 (2001).
- W. Zhou, M. S. Hurlbert, J. Schaack, K. N. Prasad, C. R. Freed, *Brain Res.* **866**, 33 (2000).
- M. B. Feany, W. W. Bender, *Nature* **404**, 394 (2000).
- P. K. Auluck, H. Y. E. Chan, J. Q. Trojanowski, V. M.-Y. Lee, N. M. Bonini, *Science* **295**, 865 (2002); published online 20 December 2001 (10.1126/science.1067389).
- M. Tanaka *et al.*, *J. Biol. Chem.* **279**, 4625 (2004).
- E. Cohen, J. Bieschke, R. M. Percivalle, J. W. Kelly, A. Dillin, *Science* **313**, 1604 (2006); published online 9 August 2006 (10.1126/science.1124646).
- P. H. Jensen *et al.*, *J. Biol. Chem.* **275**, 21500 (2000).
- M. A. Alim *et al.*, *J. Alzheimers Dis.* **6**, 435 (2004).
- Y. Kawaguchi *et al.*, *Cell* **115**, 727 (2003).
- A. Iwata, B. E. Riley, J. A. Johnston, R. R. Kopito, *J. Biol. Chem.* **280**, 40282 (2005).
- J. P. Dompiere *et al.*, *J. Neurosci.* **27**, 3571 (2007).
- Supported by a Tosteson postdoctoral fellowship award from Massachusetts Biomedical Research Corporation (T.F.O.), NIH grant 5P50-NS38372A-06 (B.T.H.), NIH grant R01-NS049221 (J.-C.R.), and a gift from Discovery of Novel Neurodegenerative Disease Therapeutics, MassGeneral Institute for Neurodegenerative Disease.

Supporting Online Material

www.sciencemag.org/cgi/content/full/1143780/DC1

Materials and Methods

Figs. S1 to S5

References

13 April 2007; accepted 8 June 2007

Published online 21 June 2007;

10.1126/science.1143780

Include this information when citing this paper.

The Near Eastern Origin of Cat Domestication

Carlos A. Driscoll,^{1,2*} Marilyn Menotti-Raymond,¹ Alfred L. Roca,³ Karsten Hupe,⁴ Warren E. Johnson,¹ Eli Geffen,⁵ Eric H. Harley,⁶ Miguel Delibes,⁷ Dominique Pontier,⁸ Andrew C. Kitchener,^{9,10} Nobuyuki Yamaguchi,² Stephen J. O'Brien,^{1,*} David W. Macdonald^{2,†}

The world's domestic cats carry patterns of sequence variation in their genome that reflect a history of domestication and breed development. A genetic assessment of 979 domestic cats and their wild progenitors—*Felis silvestris silvestris* (European wildcat), *F. s. lybica* (Near Eastern wildcat), *F. s. ornata* (central Asian wildcat), *F. s. cafra* (southern African wildcat), and *F. s. bieti* (Chinese desert cat)—indicated that each wild group represents a distinctive subspecies of *Felis silvestris*. Further analysis revealed that cats were domesticated in the Near East, probably coincident with agricultural village development in the Fertile Crescent. Domestic cats derive from at least five founders from across this region, whose descendants were transported across the world by human assistance.

The domestic cat may be the world's most numerous pet, yet little is certain of the cat's origin (1–9). Archaeological remains and anthropological clues suggest that, unlike species domesticated for agriculture (e.g., cow, pig, and sheep) or transport (horse and donkey), the cat probably began its association with humans as a commensal, feeding on the rodent pests that infested the grain stores of the first farmers (1). The earliest evidence of cat-human association involves their co-occurrence in Cyprus deposits determined to be 9500 years old (6). Domestic cats are generally considered to have descended from the Old

World wildcats, but they differ from these hypothesized progenitors in behavior, tameness, and coat color diversity (9, 10). Further, domestic cats appear to lack neotenous characteristics typical of other domesticated species (11).

Felis silvestris, from which domestic cats were derived, is classified as a polytypic wild species composed of three or more distinct interfertile subspecies: *F. s. silvestris* in Europe, *F. s. lybica* in Africa and the Near East, *F. s. ornata* in the Middle East and central Asia (1, 2, 12–15), and possibly the Chinese desert cat, *F. s. bieti* (Fig. 1A, inset). The domestic cat is sometimes

considered an additional subspecies, *F. s. catus*, possibly derived from wildcats in the Middle East or Egypt (1, 12, 14, 15). The imprecise subspecific status of *F. silvestris* populations and of the relationship of the domestic cat within this assemblage stems from morphological similarities among these groups (1, 13). A feral domestic cat with a "wild-type" mackerel tabby pattern is difficult to distinguish visually from a "true" wildcat (15, 16), which is further confounded by ongoing admixture (16–19). Moreover, the relationship between *F. silvestris* and the Chinese desert cat—which may be a

¹Laboratory of Genomic Diversity, National Cancer Institute, Frederick, MD 21702, USA. ²Wildlife Conservation Research Unit, Department of Zoology, University of Oxford, Oxford OX1 3PS, UK. ³Laboratory of Genomic Diversity, SAIC-Frederick Inc., NCI-Frederick, Frederick, MD 21702, USA. ⁴JagdEinrichtungsBüro, Am Sahlbach 9a, 37170 Fürstenhagen, Germany. ⁵Department of Zoology, Tel Aviv University, Tel Aviv 69978, Israel. ⁶Division of Chemical Pathology, University of Cape Town, Observatory 7925, Cape Town, South Africa. ⁷Department of Applied Biology, Estación Biológica de Doñana, CSIC, Avda María Luisa s/n Pabellón del Perú, 41013 Sevilla, Spain. ⁸UMR-CNRS 5558 Biométrie et Biologie Evolutive, Université Claude Bernard Lyon 1, 43 boulevard du 11 novembre 1918, 69622 Villeurbanne, France. ⁹Department of Natural Sciences, National Museums Scotland, Chambers Street, Edinburgh EH1 1JF, UK. ¹⁰Institute of Geography, School of Geosciences, University of Edinburgh, Drummond Street, Edinburgh EH8 9XP, UK.

*To whom correspondence should be addressed. E-mail: obrien@ncifcrf.gov; driscoll@ncifcrf.gov; david.macdonald@zoology.oxford.ac.uk